Affine-structure models and the pricing of energy commodity derivatives

Ioannis Kyriakou[1], Nikos K. Nomikos,

Panos K. Pouliasis and Nikos C. Papapostolou

Cass Business School, City University London

106 Bunhill Row, London EC1Y 8TZ, UK

E-mails: ioannis.kyriakou@city.ac.uk; n.nomikos@city.ac.uk;

p_pouliasis@city.ac.uk; n.papapostolou@city.ac.uk

[1]We thank Gianluca Fusai for fruitful discussions and Russell Gerrard for his valuable contribution that helped improve the paper. Versions of this paper have been presented at the Cass-ESCP 51st Meeting of the Euro Working Group on Commodities and Financial Modelling, Winter 2014 Conference of the Multinational Finance Society, 4th Energy Finance Christmas Workshop (EFC14), Energy Finance Seminar (University of Duisburg-Essen, April 2015) and Commodity Markets Workshop (Oslo, May 2015). We thank Rüdiger Kiesel, Marcel Prokopczuk and other participants for useful feedback. Usual caveat applies. Correspondence: Ioannis Kyriakou, E-mail: ioannis.kyriakou@city.ac.uk, Tel.: +44 20 7040 8738.

Abstract

We consider a seasonal mean-reverting model for energy commodity prices with jumps and Heston-type stochastic volatility, as well as three nested models for comparison. By exploiting the affine form of the log-spot models, we develop a general valuation framework for futures and discrete arithmetic Asian options. We investigate five major petroleum commodities from the European market (Brent crude oil, gasoil) and US market (light sweet crude oil, gasoline, heating oil) and analyze the effects of the competing fitted stochastic spot models in futures pricing, Asian options pricing and hedging. We find evidence that price jumps and stochastic volatility are important features of the petroleum price dynamics.

Keywords: *energy prices, affine models, futures, arithmetic Asian options, control variate Monte Carlo*

JEL classification: $G15$, $G13$, $C63$, $C13$.

1 Introduction

Understanding the stochastic process governing the energy price is essential, owing to the indispensable role of hydrocarbons in the world economy and the response of macroeconomic aggregates to oil price shocks. Concerns about the security of energy supply and the influence of geopolitical events and global economic activity on petroleum prices create the need for reliable and efficient tools to price energy-related securities and projects.

Energy commodities are predominantly different from conventional financial assets such as equity and fixed-income securities and, due to intricate price formation mechanisms, traditional modelling techniques are not directly applicable. For example, seasonal effects arise naturally from periodic supply and demand patterns[1] and have been successfully modelled by several authors including Routledge et al. (2000) and Borovkova and Geman (2006). In addition, commodity prices mean-revert to the marginal cost of production; relevant theoretical arguments and empirical evidence have been put forward by Bessembinder et al. (1995), Schwartz and Smith (2000) and Casassus and Collin-Dufresne (2005), among others. In effect, prices may temporarily be high or low, but will tend toward an equilibrium level. Furthermore, temporary supply and demand imbalances, changes in market expectations, or even unanticipated macroeconomic developments may cause sudden jumps in energy prices (Hilliard and Reis, 1998, Clewlow and Strickland, 2000). Due to construction lags on the supply side, even a relatively small change in demand can, at times, cause immediate market movements of large magnitude. Yet, jumps in returns are transient and a more persistent component may be required. In fact, compared to other markets, energy price volatility is both relatively higher and more variable over time (see, e.g., Pindyck, 2004). Trolle and Schwartz (2009) develop a stochastic volatility model for crude oil and highlight its importance in commodity derivatives pricing. Larsson and Nossman (2011) find that, in addition

[1]For example, heating oil prices experience an upward pressure during winter when storage capacity may not be able to smooth out seasonal demand shocks, particularly in the peak demand season. Instead, lower prices are anticipated during the summer inventory build-up period. On the other hand, gasoline prices typically trade at a discount during winter, as demand falls from the peak levels of the summer driving season. Crude oil demand is derived from the demand for its refined products and, as such, seasonal patterns are less evident.

to stochastic volatility, jumps are essential to capture the time series properties of oil prices. Accounting for both jumps and stochastic volatility provides a reasonable characterization of energy commodity prices in that it explains the skewness and fat-tail feature of commodity return distributions. Furthermore, it gives rise to realistic implied volatility patterns for short-term options without also affecting long-term smiles.

The previous discussion encourages the empirical testing of different spot model specifications for further use as inputs in derivatives pricing and risk management, energy investment evaluation, asset allocation and planning. The aim of this paper is to conduct a comprehensive analysis of stochastic dynamic modelling of European and US petroleum commodity prices and enrich existing literature with some new insights in several applications such as futures pricing, options pricing and hedging. In terms of scope our work shares similarities with recent contributions in the finance literature focused on other markets like, for example, the equity index (see Kaeck and Alexander, 2013), freight (see Nomikos et al., 2013) and real estate (see Fabozzi et al., 2012) markets. More specifically, we consider a seasonal mean-reverting spot price model with compound Poisson jumps and Heston-type stochastic volatility, as well as three nested models for comparison: a diffusion with stochastic volatility, a jump diffusion with constant volatility, and the classical Schwartz (1997) model with constant volatility. The Heston (1993) volatility model is both mean-reverting and positive, accounts for volatility clustering, dependence in increments and realistic implied volatility patterns. Furthermore, it allows a simple description of the correlation between the driving noises in the returns and volatility processes; in particular, positive correlation is interpreted in terms of the so-called inverse leverage effect, i.e., the observation that in commodity markets large upward price moves are associated with high volatility due to negative relationship between inventory and prices (e.g., see Pindyck, 2004, Geman, 2005).

The contribution of our paper is three-fold. Firstly, we derive the bivariate characteristic function of the suggested jump diffusion model with stochastic volatility by solving a system of Riccati equations. We then use our results to obtain expressions for the theoretical futures

prices, tackling previously noted (see Benth, 2011) mathematical challenges originated by the mean-reverting term in the price dynamics in the Heston stochastic volatility framework and rendering this useful for calibration purposes. Secondly, we fit the models to spot and futures prices of Brent crude oil and gasoil from the European market and light sweet crude oil, gasoline and heating oil from the US market. This is the first study to systematically apply a selection of stochastic models in the particular markets. We find that ignoring jumps and/or stochastic volatility leads to a less realistic description of the true data-generating process (DGP). The flexibility of the proposed general model specification is also confirmed by its ability to accurately fit the observed futures curves in the different markets. The final line of research that we contribute to in this paper relates to average (Asian) options, whose terminal payoff depends on the average level of an energy price during a pre-specified time window (e.g., see Zhang, 1995). These options are very popular in the energy commodity markets (for example, NYMEX and ICE offer several average price products linked to energy, e.g., Brent and WTI average price options) as a means of managing price exposure and potential impact on transactions, due to the time elapsed until a tanker vessel completes its route from the production site or refinery to its destination. Using our characteristic function results we obtain closed-form solutions for geometric average options, which we then use to implement efficient Monte Carlo simulation with control variates to price the more prevalent discrete arithmetic average options. This way we present a unified pricing framework under the four models considered, while extending earlier contributions by Kemna and Vorst (1990) and Fusai and Meucci (2008) based, respectively, on Gaussian and Lévy log-spot models to members from the more general affine class. The particular technique provides fast and accurate simulation outcome, which allows us to study the implications of the assumed spot price dynamics on the Asian option prices. In addition, we set up delta hedging strategies for the Asian option and investigate their performance under correct or misspecified hedges with omitted risk factors. We find that the hedging performance deteriorates in the presence of random price jumps and/or volatility. Furthermore, we find

that, under a true DGP encompassing both price jumps and stochastic volatility, which is corroborated by our analysis, a misspecified hedge that omits the jumps is closest to the true hedge.

Last but not least, we note that our proposed model framework is of chief relevance to other markets like, for example, currency and agricultural commodity markets, where the importance of stochastic volatility and/or jump risk is well-documented (e.g., see Bates, 1996, Ahlip, 2008, Geman and Nguyen, 2005, Brooks and Prokopczuk, 2013). In particular, Asian options serve as a cheaper alternative to plain vanilla options in hedging, for example, exposure to a collapse of an exchange rate; or as a means of reducing the exercise of market power by virtue of the averaging effect, for example, in agricultural commodity markets where a 'large player' can drive the market up or down affecting the payoff of an, otherwise equivalent, plain vanilla option (see Geman, 2005).

The remainder of this paper is organized as follows. In Section 2 we present our model assumptions for the dynamics of the spot energy prices. Section 3 provides a description of the data and the estimation methodology employed. Empirical results are presented in Section 4. In Section 5 we introduce our valuation framework for discrete arithmetic average options and apply in pricing and hedging. Section 6 concludes. Mathematical proofs are deferred to the appendix.

2 Model Specification and Properties

Let $(\Omega, \mathcal{F}, P)$ be a probability space equipped with filtration $\mathbb{F} := (\mathcal{F}_t)_{t>0}$. Define the commodity spot price process S as the sum of a predictable component and a stochastic component

$$S_t = f_t + \exp(X_t),\ t \geq 0.$$

The predictable component defined by the following sinusoidal function with a linear trend

$$f_t = \delta_0 + \delta_1 \sin(2\pi(t + \tau_1)) + \delta_2 \sin(4\pi(t + \tau_2)) + \delta_3 t, \tag{1}$$

with parameters $\delta_0, \delta_1, \tau_1, \delta_2, \tau_2, \delta_3$, accounts for deterministic regularities in the spot price evolution, i.e., seasonal fluctuations and time trend capturing the long-run growth in prices. Geman (2005) suggests a mean-reverting model framework for commodity spot prices with stochastic volatility. We adopt the particular model specification and extend this to accommodate sudden jumps in the prices, so that the log deseasonalized (and detrended) spot price X dynamics are given by

$$dX_t = k(\varepsilon - X_t)dt + \sqrt{V_t}dB_t + dL_t, \tag{2}$$

where k is the speed at which random shocks dissipate and process X reverts toward level ε. The evolution of the spot price variance V is modelled by the square-root diffusion as in Heston (1993), i.e.,

$$dV_t = \alpha(\beta - V_t)dt + \gamma\sqrt{V_t}dW_t \tag{3}$$

with positive parameters α (speed of variance mean-reversion), β (long-run mean variance) and γ (volatility of variance). B and W are correlated standard Brownian motions (i.e., $E(B_t W_t) = \rho t$) allowing possible inverse leverage effect, i.e., high prices associated with high volatility translating to $\rho > 0$. The spot price jump arrival is governed by the independent time-homogeneous compound Poisson process L with constant arrival rate of $\lambda > 0$ jumps (per unit time) of independent and identically normally distributed sizes J with $E(J) =: \mu_J$ and $\mathrm{Var}(J) =: \sigma_J^2$. Henceforth, we will be using the acronym MRJSV when referring to the model (2)–(3).

In this study we additionally consider three nested cases of the general model (2)–(3) depending on the assumptions on the spot price jumps and volatility:

MRSV: diffusion model ($dL_t = 0$ for all t) with Heston stochastic volatility.

MRJ: jump diffusion model with constant volatility $\sqrt{V_t} = \sigma$ for all t.

MR: Schwartz dynamics with $dL_t = 0$ and $\sqrt{V_t} = \sigma$ for all t.

In Sections 3 and 5 we derive futures and option prices based on our proposed model framework. For this purpose, we require risk neutral dynamics for the spot price. Following Benth (2011) we employ standard change of measure with respect to the Brownian motion driving the spot price dynamics

$$d\tilde{B}_t := dB_t + \frac{h}{\sqrt{V_t}}dt,$$

where h is the (constant) market price of risk. Note that one may also introduce a change of measure in the volatility dynamics; we do not consider this here but, instead, as we explain in Section 3, we calibrate the stochastic volatility model to market prices of traded futures contracts. A measure-change with respect to the jump process L is also not considered.

MRJSV belongs to the class of affine-structure models (see Duffie et al., 2000 and Duffie et al., 2003), hence the characteristic function $\phi_{V,X}(t, u_1, u_2) := E\left(\exp\left\{iu_1V_t + iu_2X_t\right\}\right)$ has exponentially affine dependence on V and X, i.e., there exist functions $\psi_0, \psi_1, \psi_2 : \mathbb{R}_+ \times \mathbb{R}^2 \to \mathbb{C}$ so that

$$\phi_{V,X}(t, u_1, u_2) = \exp\left\{\psi_J(t, u_2) + \psi_0(t, u_1, u_2) + \psi_1(t, u_1, u_2)V_0 + \psi_2(t, u_1, u_2)X_0\right\}, \qquad (4)$$

where

$$\psi_J(t, u_2) := \lambda t\left(e^{iu_2\mu_J - \frac{1}{2}\sigma_J^2u_2^2} - 1\right)$$

and ψ_0, ψ_1, ψ_2 satisfy the system of Riccati equations

$$\begin{aligned}
\frac{\partial \psi_2}{\partial t} &= -k\psi_2, && (5)\\
\frac{\partial \psi_1}{\partial t} &= -\alpha\psi_1 + \frac{1}{2}\gamma^2\psi_1^2 + \rho\gamma\psi_1\psi_2 + \frac{1}{2}\psi_2^2, && (6)\\
\frac{\partial \psi_0}{\partial t} &= \alpha\beta\psi_1 + k(\varepsilon - h/k)\psi_2, && (7)
\end{aligned}$$

subject to the boundary conditions

$$\psi_0(0, u_1, u_2) = 0, \quad \psi_1(0, u_1, u_2) = iu_1, \quad \psi_2(0, u_1, u_2) = iu_2.$$

By straightforward integration of (5) and (7) we get that

$$\psi_2(t, u_1, u_2) = iu_2 e^{-kt} \tag{8}$$

and

$$\psi_0(t, u_1, u_2) = \alpha\beta \int_0^t \psi_1(s, u_1, u_2)ds + iu_2(\varepsilon - h/k)(1 - e^{-kt}),$$

respectively. Solving (6) explicitly is not trivial; from Proposition 3 (see Appendix A.1), the general solution to (6) is given by (A.3)

$$\psi_1(t, u_1, u_2) = -\frac{2iu_2k}{\gamma^2}e^{-kt}\zeta(iu_2e^{-kt}) + \frac{M(t, u_2)}{C(u_1, u_2) - \frac{1}{2}\gamma^2\int_0^t M(s, u_2)ds},$$

where M is defined in (A.6) and

$$C(u_1, u_2) := \frac{\exp\left(-\frac{iu_2\rho\gamma}{k} + 2\int_0^{iu_2}\zeta(y)dy\right)}{iu_1 + \frac{2iu_2k}{\gamma^2}\zeta(iu_2)}$$

satisfies $\psi_1(0, u_1, u_2) = iu_1$. Function ζ, which satisfies Eq. (A.1), admits the representation

$$\zeta(y) = \sum\nolimits_{j=1}^{\infty} d_j y^j,$$

where the coefficients $\{d_j\}_{j=1}^{\infty}$ satisfy the recursion

$$\left(j+1-\frac{\alpha-k}{k}\right)d_{j+1}=\sum\nolimits_{i=1}^{j-1}d_i d_{j-i}\mathbf{1}_{j>1}-\frac{\rho\gamma}{k}d_j\mathbf{1}_{j>0}+\frac{\gamma^2}{4k^2}\mathbf{1}_{j=0}.$$

(Alternatively, one may consider solving (6) numerically using, e.g., Matlab built-in solvers, however, at increased computational cost.)

In the case of the one-dimensional MRJ model with constant volatility σ, the characteristic function $\phi_X(t,u):=E\left(e^{iuX_t}\right)$ takes the simplified form

$$\phi_X(t,u)=\exp\left\{\psi_J(t,u)+iu(\varepsilon-h/k)(1-e^{-kt})-\frac{\sigma^2u^2}{4k}(1-e^{-2kt})+iue^{-kt}X_0\right\} \qquad (9)$$

(see Cont and Tankov, 2004), whereas in the cases of the MRSV and MR models the characteristic functions of (V,X) and X, respectively, follow directly from (4) and (9) for $\lambda=0$.

3 Data and Estimation Methodology

In this study we consider five energy commodities: two representatives of the European petroleum market and three from the US market. European spot prices are the dated Brent (CB), which serves as a benchmark assessment of the price of physical light crude oil in the North Sea, and the gasoil (GO) European Economic Community Cost in North West Europe; corresponding futures contracts are traded on the Intercontinental Exchange (ICE Futures Europe). US spot prices are the light sweet crude oil WTI (CL) at Cushing, Oklahoma, RBOB gasoline (HU), and No. 2 heating oil (HO) in New York harbor; corresponding futures are traded on NYMEX of the CME Group. For the purposes of our study we use a time series of constant-maturity futures; the futures curve is constructed by cubic spline interpolation of market prices of traded futures contracts. Volume and open interest data lead us to consider a block of 12 contracts for each commodity from 1 up to 12 months to maturity. The choice of constant-maturity contracts ensures that all prices are measured

at the same point in time avoiding problems related to thin trading, expiration effects and discontinuities from rolling over futures contracts. We consider a 4-year period from March $12, 2009$ to March $11, 2013$, that is, a total of $1,043$ daily observations after the necessary refinements for bank holidays. Data are collected from Datastream.

We use daily historical spot price data to estimate the predictable component (1) for each commodity. We then employ a two-stage estimation procedure based on Clewlow and Strickland (2000), Benth (2011) and Broadie et al. (2007). First, using the log deseasonalized spot price time series, we obtain the spot parameter estimates of the MRJSV and nested MRSV, MRJ, MR models of Section 2 by recursive filtering. Given these, in the second stage we use the information embedded in end-of-day futures contract quotes to estimate the volatility parameters and the market price of risk.

In more details, we define a jump as an observation in the log deseasonalized price changes series that is greater in absolute value than a market-specific threshold given by a multiple of the sample standard deviation of the deseasonalized series (see Clewlow and Strickland, 2000). The prices on the identified 'jump dates' are substituted by the averages of the two adjacent prices, the standard deviation of the updated series is recalculated and the same procedure is repeated until no more jumps are identified[2]. We then estimate the jump arrival rate λ by the average number of identified jumps per year; the estimates of the mean μ_J and standard deviation σ_J of the jump size distribution are given by the average and standard deviation of the jump returns, respectively[3]; parameters k and ε of the spot model are estimated using OLS regression. In order to calibrate the remaining parameters, i.e., the

[2]We choose the threshold (multiple m of the sample standard deviation) that leads to the best calibrated model, i.e., the one that minimizes the Jarque and Bera (1980) statistic of the filtered series (ensures that daily log-price changes are closest to the normal distribution). To this end, we implement the jump-removal procedure for different multiples $m = 0.5 + k/100$, $k = 0, \ldots, 450$, and find that the optimal multiples m^* are for each market 2.8 (CB), 2.75 (GO), 2.7 (CL), 2.7 (HU) and 2.8 (HO).

[3]Empirical evidence suggests that the Clewlow–Strickland recursive-filtering approach can be superior to the common alternative, that is, the maximum likelihood method in estimating jump parameters in the case of infrequent and highly volatile jumps usually observed in energy markets; in particular, Nomikos and Andriosopoulos (2012) find that the maximum likelihood method results in understated jump size volatility and mean magnitude and overstated jump frequency. Variants of the filtering approach have also been adopted by several authors including, for example, Borovkova and Permana (2006) and Geman and Roncoroni (2006).

variance model parameters α, β, γ, the correlation coefficient ρ and the market price of risk h, we use end-of-day futures contract quotes. This is possible given explicit expressions for the futures price F under the different model specifications.

Proposition 1 *The futures price $F(0,T)$ at time 0 for a contract expiring at time $T > 0$ is given by*

$$F(0,T) = E(S_T) = f(T) + E(e^{X_T}),$$

where

$$E(e^{X_T}) = \begin{cases} \phi_{V,X}(T,0,-i), & \textit{under MRJSV (and MRSV with } \lambda = 0\textit{)} \\ \phi_X(T,-i), & \textit{under MRJ (and MR with } \lambda = 0\textit{)} \end{cases}.$$

Proof. Follows from (4) and (9). ■

Let $F_{j,l}$ be the observed futures prices at time t_j of a contract maturing at T_l. The theoretical futures price $F_\theta(t_j, T_l)$ is given in Proposition 1; $F_\theta(t_j, T_l)$ depends on the observed log deseasonalized spot price time series $\{X_j\}_{j=1}^n$, the unobserved variance series $\{V_j\}_{j=1}^n$ which we approximate by the (conditional) expected variance $\{\hat{V}_j\}_{j=1}^n$ where $\hat{V}_j := \beta + (\hat{V}_{j-1} - \beta)e^{-\alpha/264}$ with unknown $\hat{V}_1$ to be estimated, and the parameter vector $\theta := (\hat{V}_1, \alpha, \beta, \gamma, \rho, h)$. We obtain θ by minimizing the Euclidean distance between the observed and theoretical futures prices

$$\theta^* := \arg\min_\theta \sum\nolimits_{j=1}^{n} \sum\nolimits_{l=1}^{m} \sqrt{|F_{j,l} - F_\theta(t_j, T_l)|^2}, \tag{10}$$

where $m = 12$ is the number of maturities and $n = 1,043$ the number of days in the sample.

4 Empirical Results

In this section we discuss the estimation results of the four model specifications MRJSV, MRSV, MRJ and MR for each of the CB, GO, CL, HU and HO markets. We begin the analysis with the calibration results. We then test the performance of the different spot

models in commodity futures pricing. By means of a simulation study, we further examine if the specified models can accurately represent the true spot price dynamics[4].

4.1 Model Calibration

We fit first the predictable component (1) with a trend and two terms capturing annual and semi-annual seasonal cycles; standard likelihood ratio test leads to acceptance of the hypothesis of both annual and semi-annual seasonality at the 5% significance level for all markets. The estimated parameters are reported in Panel A of Table 1 along with their standard errors. Results suggest that all markets exhibit significant regularities: adjusted $\bar{R}^2$ are 76% and 82% for the European CB and GO, and 59%, 79% and 83% for the US CL, HU and HO.

Next, we employ the estimation procedure described in Section 3. Parameter estimates with standard errors are reported in Panel B of Table 1. Several remarks are in order. Parameter k estimates imply that the expected time for the log deseasonalized spot prices to return half way toward level ε is 51 days (half-life $k^{-1}\ln 2$), on average, for the European markets (CB and GO) and 35 days for the US markets (CL, HU and HO); inclusion of jumps in the spot price model results in increased half-lives of 55 and 44 days, respectively, as jump returns are less persistent. Jumps are infrequent events and tend to be negative. More specifically, we find that jumps in the European markets are less frequent, i.e., expected 3.2-3.4 jumps per year for GO and CB versus 4.6-5.0 for HO and CL and 7.6 for HU, and have smaller standard deviation, i.e., 6.4%-6.7% for CB and GO versus 7.7%-7.9% for CL and HO and 9.2% for HU. The relative importance of the jump component is also evident by its percentage contribution to the total variance of the fitted spot model, which lies in

[4]Throughout the paper, we consider the following sample-path generation techniques for the MR, MRSV, MRJ and MRJSV models: MR trajectories are simulated using standard exact methodology described, for example, in Glasserman (2004, Section 3.3). MRSV log-spot price trajectories are simulated based on the central-discretization method of Andersen (2008); for the simulation of the stochastic variance paths we employ the method described in Glasserman (2004, Section 3.4) (for a faster simulation, one can alternatively use the low-bias quadratic-exponential method of Andersen, 2008). Finally, for the compound Poisson jumps in the MRJ and MRJSV models, we use the improved algorithm in Cont and Tankov (2004, Section 6.1). For more details about the actual implementation of the simulation schemes, see steps 1–3 in Table 3.

12%-13% for CB and GO, 19%-21% for CL and HO, and 29% for HU.

Turning next to the volatility model parameters, in the case of the MRSV model the estimated speeds of variance mean-reversion translate to average half-lives ($\alpha^{-1}\ln 2$) of 5.2 (CB and GO) and 3.6 days (CL, HU and HO). In general, the long-run mean variance, volatility of variance and the correlation between log-prices and variance innovations are lower for the European CB and GO than for the US CL, HO and HU. We note that the correlation is found positive in consistency with the inverse leverage effect in energy prices, meaning that high prices are associated with high volatility, which can be attributed to the negative relationship between prices and inventory (e.g., see Pindyck, 2004). Incorporating price jumps (i.e., case of the MRJSV model) has a downward effect on the speed of variance mean-reversion, long-run mean variance, volatility of variance and correlation level, as the need for the variance process to create large sudden movements becomes less important.

In addition, we compute the root mean square error (RMSE) and relative RMSE (RRMSE) of the model-implied theoretical futures prices given in Proposition 1 for each model with respect to the observed futures prices: RMSE $:= \sqrt{\frac{1}{nm}\sum_{j=1}^{n}\sum_{l=1}^{m}\left|F_{\theta^*}(t_j,T_l)-F_{j,l}\right|^2}$ and RRMSE $:= \sqrt{\frac{1}{nm}\sum_{j=1}^{n}\sum_{l=1}^{m}\left|F_{\theta^*}(t_j,T_l)/F_{j,l}-1\right|^2}$, where $F_{j,l}$ is the observed futures prices at time t_j of a contract maturing at T_l, $F(t_j,T_l)$ is the theoretical futures price given in Proposition 1 for each model under the optimal parameter set θ^* (see Eq. 10), $m = 12$ (no. of maturities) and $n = 1,043$ (no. of days in the sample period March 12, 2009 to March 11, 2013). Results presented in Panel C of Table 1 suggest that MRJSV generates lowest pricing error: across markets, average RRMSE is 13% and maximum RRMSE is 16% (HU). (We reach similar conclusion if we consider the mean absolute percentage error MAPE $:= \frac{1}{nm}\sum_{j=1}^{n}\sum_{l=1}^{m}\left|F_{\theta^*}(t_j,T_l)/F_{j,l}-1\right|$; results are currently not presented for brevity.) To test whether any of the extended versions of the basic MR model with price jumps and/or stochastic volatility yields significant improvement in the futures pricing performance, we apply the Hansen (2005) test[5]. We find that accurately modelling jumps in the

[5]We define loss function (LF) differentials between the MR model and each of the MRSV, MRJ and MRJSV models based on the RMSE and RRMSE error statistics, e.g., $\mathrm{LF}_{t_j} = \mathrm{RMSE}_{\mathrm{MR},t_j} - \mathrm{RMSE}_{\mathrm{MRJSV},t_j}$

spot price dynamics improves satisfactorily the fit of the resulting theoretical futures prices to the observed futures prices compared to the MR model; admitting additionally stochastic volatility improves the fit further. More specifically, compared to MR, MRJSV provides a 4% average, across markets, reduction in the RMSE. Unsurprisingly, highest reduction, that is, 6.3%, is reported in the HU market having the most frequent price jumps, highest jump size standard deviation, volatility of variance and correlation between variance and log-price processes. The improvement in the fit brought by MRJSV compared to MRSV is still high, that is, 2.1% average reduction in the RMSE, whereas compared to MRJ the RMSE reduction is up to 1%.

We conclude this analysis by referring to an additional error statistic, that is, the mean percentage error MPE $:= \frac{1}{nm}\sum_{j=1}^{n}\sum_{l=1}^{m}(F_{\theta^*}(t_j,T_l)/F_{j,l}-1)$, which we compute for the entire term structure of futures prices and use to test for systematic bias. The outcome of the test suggests rejection of this hypothesis at conventional significance levels. For brevity we do not detail these results here, but we can make these available upon request.

4.2 Simulation Study: True Data-Generating Process

As a next stage in our analysis, we examine whether the proposed models can accurately represent the true price dynamics of the commodities of interest. Similarly to Kaeck and Alexander (2013), we compare the model-implied distributions to the empirical one for each commodity in terms of a set of statistics. We employ the following test procedure: for each commodity we approximate the empirical distribution of the log-returns using stationary bootstrap and construct 90% bootstrap confidence intervals for the standard deviation, skewness, kurtosis, 1st and 99th percentiles and expected shortfalls at the 1% and 99% levels. Then, for each model, we simulate $100,000$ price paths and log-return sample statistics, and calculate the percentage number of simulated statistics of a given type falling within the

where $j = 1,\ldots,n = 1,043$. Then, using $5,000$ bootstrap simulations, we test the null hypothesis that MR is not outperformed by the other models, i.e., $H_0 : E(\mathrm{LF}) \leq 0$. For more details, we refer to White (2000) and Hansen (2005); a description of the stationary bootstrap algorithm can also be found in Politis and Romano (1994) and Sullivan et al. (1999, Appendix C).

corresponding bootstrap confidence interval; a value closer to 1 implies smaller discrepancy between the observed and assumed price dynamics. The model with the best relative performance for given statistic type is indicated by an asterisk in Table 2. If we take a close look at the table, we see that, although the MR model appears to be fitting well the standard deviation and the 99th percentile (65% and 89%, respectively, of the time on average across markets), it naturally does not capture the skewness and kurtosis (33% and 10%, respectively) of the empirical distribution. As a result, the left tail is missed more often in the case of MR (and MRSV but to a lesser extent). On the other hand, including jumps (i.e., case of MRJ and MRJSV models) allows a more balanced and thus accurate fitting of the tails, adequately accounting for both the skewness and excess kurtosis commonly found in commodity log-returns. In particular, comparing model-implied standard deviation, skewness and kurtosis across the five markets for each model, we observe that MRJSV produces more realistic statistics in 10 cases out of 15 (3 statistics $\times$ 5 markets). The 1st and 99th percentiles as well as the expected shortfalls at the 1% and 99% levels of the empirical and model-implied log-return distributions are also reported suggesting overall superiority of the MRJSV model in 10 out of 20 cases.

In addition, we employ the two-sample Kolmogorov–Smirnov test with the null hypothesis stating that the observed and simulated log-return distributions are equal. To this end, for each of the simulated price paths of the competing models, we test the null hypothesis and store the p-value. Table 2 reports the percentage number of times the null hypothesis cannot be rejected at the 10% significance level. In the case of the MR model the null hypothesis cannot be rejected in 62.1% (CB), 56.5% (GO), 55.1% (CL), 35.7% (HO) and 59.7% (HU) of the simulation runs. Accounting for price jumps or stochastic volatility (i.e., MRJ or MRSV model) raises the evidence in favour of the null hypothesis, while the combined effect (i.e., case of MRJSV model) is found strongest with non-rejection in 88.4% (CB), 92.8% (GO), 82.1% (CL), 84.4% (HO) and 80.1% (HU) of the time.

Overall, we find that the MRJSV model is sufficiently rich and capable of providing a

more realistic description of the true DGP, accounting for the stylized patterns of the spot prices in the petroleum markets under consideration.

5 Application on Discrete Arithmetic Asian Options

In what follows we investigate the impact of the proposed stochastic models in Section 2 in terms of the pricing and delta hedging of options on the discrete arithmetic average spot price, which are particularly popular in commodity markets. The need for realistic spot price models capturing the unique characteristics of energy commodities raises substantially the complexity of the option pricing problem. We solve this by means of an efficient Monte Carlo simulation approach, which we develop based on the model properties presented in Section 2. We then execute pricing and delta hedging simulation exercises based on the calibrated model parameters in Section 4.

5.1 Option Pricing

Suppose that the spot price S is monitored over the period $[0, T]$, $T > 0$, at the following equidistant dates: $0, \delta, \ldots, j\delta, \ldots, n\delta = T$.

The terminal payoff of the arithmetic Asian option depends on the average of the past $n + 1$ spot prices

$$\frac{1}{n+1}\sum\nolimits_{j=0}^{n} S_{j\delta} = A_{n+1} + \frac{1}{n+1}\sum\nolimits_{j=0}^{n} f_{j\delta},$$

where f is given by (1) and

$$A_{n+1} := \frac{1}{n+1}\sum\nolimits_{j=0}^{n}(S_{j\delta} - f_{j\delta}) = \frac{1}{n+1}\sum\nolimits_{j=0}^{n} e^{X_{j\delta}}$$

is the average deseasonalized spot price. The price of the arithmetic Asian call option with

fixed strike price K reads

$$E\left[e^{-rT}\left(\frac{1}{n+1}\sum\nolimits_{j=0}^{n} S_{j\delta} - K\right)^{+}\right] = E\left[e^{-rT}\left(A_{n+1} - \tilde{K}\right)^{+}\right], \tag{11}$$

where $x^{+} := \max(x, 0)$,

$$\tilde{K} := K - \sum\nolimits_{j=0}^{n} f_{j\delta}/(n+1)$$

is the deseasonalized strike price, and r the continuously compounded risk free rate of interest. Note that the price of the put-type option can be obtained via standard put-call parity. By analogy, the price of the Asian call option on the geometric average spot price is given by

$$E\left[e^{-rT}\left(e^{Y_{n+1}} - \tilde{K}\right)^{+}\right], \tag{12}$$

where

$$Y_{n+1} := \frac{1}{n+1}\sum\nolimits_{j=0}^{n} \ln(S_{j\delta} - f_{j\delta}) = \frac{1}{n+1}\sum\nolimits_{j=0}^{n} X_{j\delta}. \tag{13}$$

For the purposes of our analysis, we estimate the price of the arithmetic option, i.e., evaluate (11), by employing an accurate control variate Monte Carlo (CVMC) scheme with $100,000$ simulations and the geometric Asian option price (12) used as control variate (see Table 3 and Glasserman, 2004 for more details). Given the exact closed-form expression for the price of the geometric option under Black–Scholes–Merton model assumptions, Kemna and Vorst (1990) show that the geometric option serves as an efficient control variate in the simulation of the arithmetic option. Fusai and Meucci (2008) extend to Lévy log-spot models by adopting a Fourier transform approach, whereas in this paper we generalize to non-Lévy members of the affine class, including the MRJSV model and the nested models of Section 2. To this end, we derive first the characteristic function of the log-geometric average, $\phi_{Y_{n+1}}(u) := E\left(\exp\{iuY_{n+1}\}\right)$, under the given model assumptions.

Proposition 2 *The characteristic function of the log-geometric average Y_{n+1} defined in (13) is given:*

(a) under the MRJSV model dynamics by

$$\phi_{Y_{n+1}}(u) = \exp\left\{\sum\nolimits_{j=1}^{n}\left(\psi_J(\delta,\vartheta_j)+\psi_0(\delta,\eta_j,\vartheta_j)\right)+\psi_1(\delta,\eta_1,\vartheta_1)V_0+i\vartheta_0 X_0\right\}, \quad (14)$$

where $\eta_n := 0$, $\vartheta_n := u/(n+1)$, $\eta_j := -i\psi_1(\delta,\eta_{j+1},\vartheta_{j+1})$ *and* $\vartheta_j := -i\psi_2(\delta,\eta_{j+1},\vartheta_{j+1})+u/(n+1)$ *for* $0 \le j \le n-1$.

(b) under the MRJ model dynamics by

$$\begin{aligned}\phi_{Y_{n+1}}(u) &= \prod\nolimits_{j=0}^{n}\exp\left\{\frac{iu}{n+1}X_0 e^{-kj\delta}\right\} \\ &\quad\times\prod\nolimits_{j=1}^{n}\exp\left\{\psi_J(\delta,\eta_j)+i\eta_j(\varepsilon-h/k)(1-e^{-k\delta})-\frac{\sigma^2\eta_j^2}{4k}(1-e^{-2k\delta})\right\},\end{aligned}$$

where $\eta_j := u\sum_{m=0}^{n-j}e^{-mk\delta}/(n+1)$ *for* $0 < j \le n$.

Relevant results under the MRSV and MR models follow directly by setting $\lambda = 0$.

Proof. See Appendix A.2. ■

Given the characteristic function of the log-geometric average, the exact price of the geometric Asian option (12) can be computed by means of the Fourier-inversion formula with respect to the log-strike price $\tilde{\kappa} := \ln\tilde{K}$

$$E\left[e^{-rT}\left(e^{Y_{n+1}}-\tilde{K}\right)^{+}\right] = \frac{e^{-\xi\tilde{\kappa}-rT}}{2\pi}\int_{\mathbb{R}}e^{-iu\tilde{\kappa}}\frac{\phi_{Y_{n+1}}(u-\xi i-i)}{(iu+\xi)(iu+\xi+1)}du, \quad (15)$$

where constant $\xi > 0$ ensures integrability in $\tilde{\kappa}$ (see Carr and Madan, 1999). Formula (15) can be evaluated using the (fractional) fast Fourier transform algorithm (e.g., `fft` or `czt` in Matlab, see Černý and Kyriakou, 2011 for more details) which outputs the geometric Asian option prices on a fine, equally spaced grid of log-strike prices.

Based on the estimated model parameters (see Table 1) and using our results for the geometric Asian option, we implement standard CVMC setup (see Table 3) to estimate the prices of at-the-money (ATM), in-the-money (ITM) and out-of-the-money (OTM) 1-month

to maturity arithmetic Asian call options with daily monitoring (i.e., $n = 22$). In particular, the strike price is set equal to 100%, 95% and 105% of the spot price. The current spot price and variance are set equal to $\exp(\varepsilon)$ and β, respectively, and the risk free interest rate is given by the average 3-month US T-bill rate throughout the sample period. Computed option prices are presented in Table 4 in monetary terms (CB - \$/bbl, GO - \$/mt, CL - \$/bbl, HU - c\$/gal, HO - c\$/gal) as well as relative to the spot price and the price of the corresponding ATM option.

Results suggest that ignoring jumps and stochastic volatility leads to lower option prices. More specifically, we find that, across all markets, MRSV and MRJSV prices are systematically higher than the corresponding MRJ prices, which, further, are higher than the MR ones. In fact, the discrepancies between MRSV, MRJSV and MRJ prices versus MR prices are higher for in-the-money options, whereas these reduce the more out-of-the-money the option. Our observation based on option prices under non-Lévy (i.e., dependent) log-returns adds to earlier contributions by Fusai and Meucci (2008) and Černý and Kyriakou (2011), who observe similar pattern across different level of moneyness based on option prices relying on Lévy (i.e., independent) assumptions for stock log-returns. As noted in Černý and Kyriakou (2011), such pattern is attributed to the combined kurtosis-skewness effect in a Lévy and non-Lévy, as opposed to normal, log-return distribution.

5.2 Hedge Performance Comparisons

The MRJ, MRSV and MRJSV models we have considered in this paper generally correspond to incomplete markets due to the presence of stochastic jumps and/or volatility, thus introducing a hedging error in a delta hedging strategy even in the theoretical limit of continuous rebalancing as the two instruments (the underlying and the risk free bond) are not enough to span the sources of uncertainty. In the case of the one-factor MR diffusion, existence of error can be attributed to the discreteness of the portfolio rebalancing frequency. In what follows, we adhere to the common market practice of delta hedging and apply to the case of Asian

options and inspect the performance of the delta hedge in the various markets. We define the hedging error as the difference between the value of the daily-rebalanced hedge portfolio and the value of a 1-month to maturity, daily-averaged ATM arithmetic Asian option for a 1-week hedge period.

We use Monte Carlo simulation to gauge the magnitude and distributional characteristics of the hedging error. For each commodity we simulate the distribution of the hedging error when the underlying data-generating process is given by either of the MR, MRJ, MRSV and MRJSV models and (a) the hedge portfolios are formed accordingly, or (b) the hedge portfolios are misspecified, i.e., are formed based on alternative models. In fact, case (b) is more realistic as the hedger never really knows the true DGP, hence develops the hedging approach based on some assumptions. The particular task allows us to investigate the sensitivity of the hedging performance to model misspecification, in other words, the impact of incorrectly specifying the underlying data-generating process and forming the hedge portfolios. In simulating the hedging error distributions under the dynamic strategy, the option prices are estimated daily using the CVMC approach in Section 5.1, whereas the option deltas using a modified version based on straightforward application of the pathwise technique (see Glasserman, 2004) with the geometric Asian option delta used as control variate.

We consider first computed hedging errors under each driving process with the hedge portfolios formed accordingly. Figure 1 plots the simulated price paths of each underlying commodity across the 5-day hedge period coupled with the hedging error distributions at the closing of the week-long hedging exercise, under the four data-generating processes. Most of the hedging errors are negative, irrespective of the direction of the moves in the price of the underlying. As discussed in Carr and Wu (2014), the reason is that the option price exhibits convexity with the price of the underlying, resulting in the value of the delta neutral portfolio being below the value of the option contract under sufficiently large price movements. Similarly to their dynamic hedging exercise, this effect becomes more pronounced

when jumps are allowed, and therefore larger moves in the price of the underlying, as in our MRJ and MRJSV models. Our results are consistent with those of Carr and Wu (2014) in the sense of achieving negative skewness of hedging error and positive excess kurtosis, even in the case of the underlying price moving purely diffusively; as shown in Figure 1, this effect becomes more perceptible when discontinuities are allowed in the price dynamics. This also explains the negative mean hedging error reported in Panel A of Table 5 across all markets and models (see also Brooks and Prokopczuk, 2013 for the case of European options), although expectedly this is smaller (in absolute value) in the case of the pure diffusion model. Models with jumps and/or stochastic volatility generate hedging errors with increased standard deviation compared to the basic one-factor model. Therefore, the performance of the delta hedge deteriorates when more than one risk factors are allowed.

In the event of model misspecification, the investor's hedge model deviates from the true model. Panel B of Table 5 reports the percentage changes in the standard deviation of the hedging error under different misspecified hedge portfolios, allowing us to explore the effect of model uncertainty on the hedging error. More specifically, we consider incorrect hedges containing fewer risk factors than the true model, i.e., the misspecified hedge model either omits the jump component, the stochastic volatility, or both. Incorrect hedges in this case always result in increased standard deviation of the hedging error (positive entries in Panel B). When the MRJSV model represents the true DGP (Panel B.3), as also corroborated by our analysis in Section 4, we find that the misspecified MRSV hedge performs better achieving lowest increase of standard deviation in the GO, CL, HU and HO markets, the CB market being the only exception in which case the MRJ hedge is slightly better. Therefore, we find that the hedge model with stochastic volatility is closest to the true hedge. Our observation is consistent with the remarks of Branger et al. (2012) based on the analysis of different hedging strategies for plain vanilla stock options. It is worth noting that we do not consider the opposite situation, i.e., hedge models with more risk factors than the true one, which is not practically relevant as the true data-generating process is usually more

complicated and involves many risk factors while investors are simpler than 'real life' (see Branger et al., 2012).

Finally, we perform a robustness check of the outcome of the hedging exercise. We perturb each of the parameters by $\pm 1\%$ from their original estimates and study the impact on the variance of the hedging error. Through this sensitivity analysis, we reach that the signs of the entries in Table 5 remain unchanged. Further research toward this direction could include, for example, a study of the distribution of the variance (and possibly higher moments) of the hedging error under parameter resampling; this is a nontrivial and particularly computationally intensive problem at this stage, due to the extremely large number of simulations required, whose further investigation is left for future research.

6 Summary and Conclusion

We have considered five major European and US petroleum commodity markets to study the ability of four different model specifications to realistically portray the dynamics of the data-generating process using historical spot and futures price data over the period March 2009 to March 2013. Our selection of models includes a seasonal mean-reverting spot price model with jumps and Heston-type stochastic volatility (MRJSV) and nested specifications with/out jumps or stochastic volatility (MR, MRJ, MRSV). In the first stage of our analysis, we assess relative performance by comparing simulated model-implied and empirically estimated statistics as well as testing for equality of the observed and simulated log-return distributions; our exercise indicates superior performance of the MRJSV model in producing dynamics that are similar to the true price dynamics. Furthermore, using the theoretical futures prices derived for all competing models, we investigate the fit to the observed futures curves in the different markets; our error statistics point toward inclusion of price jumps, while combining with stochastic price volatility improves the fit further.

In addition, given the widespread use of Asian options in commodity markets, we provide an efficient valuation framework for the prevalent case of the arithmetic average with discrete

monitoring when the underlying spot is driven by a general exponential affine model. Our findings suggest that failing to account for price jumps and stochastic volatility leads to relatively lower option premia, especially for in-the-money call options. Furthermore, we gauge the distributional characteristics of the hedging error from dynamic delta hedging strategies applied to an Asian option. In the case of an investor with perfect knowledge of the stochastic process governing the underlying asset price, the performance of the hedging strategy deteriorates in the presence of random price jumps and/or volatility. The delta hedge becomes even more ineffective in the case of incorrectly specified hedges with omitted risk factors. We find that when the MRJSV model represents the true DGP, as corroborated by our analysis in Section 4, a misspecified hedge with omitted jumps but allowed stochastic volatility is closest to the true hedge.

The implications of this research are of chief relevance to market participants, as specifying correctly the dynamic behaviour of the underlying spot price process is important for understanding and managing the risks associated with derivative securities, investment evaluation, asset allocation and planning.

Appendix A: Proofs

A.1 Proof of general solution to Riccati equation (6)

Proposition 3 *Suppose* $\zeta(y)$, $y \in \mathbb{C}\backslash\{0\}$, *satisfies the equation*

$$\zeta'(y) = \zeta(y)^2 + \left(\frac{\alpha - k}{ky} - \frac{\rho\gamma}{k}\right)\zeta(y) + \frac{\gamma^2}{4k^2}. \tag{A.1}$$

Define

$$\chi(t, u_2) = -\frac{2iu_2k}{\gamma^2}e^{-kt}\zeta(iu_2e^{-kt}). \tag{A.2}$$

Then,

(a) χ *is a solution to (6).*

(b) the general solution to (6) takes the form

$$\psi_1 = \chi + \frac{1}{w}, \tag{A.3}$$

where w satisfies the differential equation

$$\frac{\partial w}{\partial t} + \left(-\alpha + iu_2\rho\gamma e^{-kt} + \gamma^2\chi\right) w = -\frac{1}{2}\gamma^2. \tag{A.4}$$

Proof.

(a) From (A.2), we obtain

$$\begin{aligned}
\frac{\partial \chi}{\partial t} &= -k\chi - \frac{2u_2^2k^2}{\gamma^2}e^{-2kt}\zeta'(iu_2e^{-kt}) \\
&= -k\chi - \frac{2u_2^2k^2}{\gamma^2}e^{-2kt}\left[\zeta(iu_2e^{-kt})^2 + \left(\frac{\alpha - k}{iu_2ke^{-kt}} - \frac{\rho\gamma}{k}\right)\zeta(iu_2e^{-kt}) + \frac{\gamma^2}{4k^2}\right] \\
&= -\alpha\chi + \frac{1}{2}\gamma^2\chi^2 + \rho\gamma\chi\psi_2 + \frac{1}{2}\psi_2^2,
\end{aligned} \tag{A.5}$$

where the second equality follows from (A.1) and ψ_2 in the last equality is given by (8). It is implied from (A.5) that χ is a solution to (6).

(b) Suppose that $\chi + 1/w$ is an arbitrary solution to (6). Then we have

$$\frac{\partial \chi}{\partial t} - \frac{1}{w^2}\frac{\partial w}{\partial t} = -\alpha\left(\chi + \frac{1}{w}\right) + \frac{1}{2}\gamma^2\left(\chi^2 + \frac{2\chi}{w} + \frac{1}{w^2}\right) + \rho\gamma\left(\chi + \frac{1}{w}\right)\psi_2 + \frac{1}{2}\psi_2^2$$

and, further, from (A.5) we get

$$-\frac{1}{w^2}\frac{\partial w}{\partial t} = -\frac{\alpha}{w} + \frac{1}{2}\gamma^2\left(\frac{2\chi}{w} + \frac{1}{w^2}\right) + \frac{\rho\gamma\psi_2}{w},$$

from which (A.4) follows.

■

For the differential equation (A.4) with χ given in (A.2), from standard calculus theory the integrating factor is

$$\begin{aligned} M(t) &:= \exp\left(-\alpha t - \frac{iu_2\rho\gamma}{k}e^{-kt} - 2iu_2k\int e^{-kt}\zeta(iu_2e^{-kt})dt\right) \\ &= \exp\left(-\alpha t - \frac{iu_2\rho\gamma}{k}e^{-kt} + 2\int_0^{iu_2e^{-kt}}\zeta(y)dy\right), \end{aligned} \tag{A.6}$$

from which we get the general solution to (A.4)

$$w(t) = \frac{C - \frac{1}{2}\gamma^2\int_0^t M(s)ds}{M(t)}$$

where C is the constant of integration.

A.2 Proof of Proposition 2

Proof.

(a) Under the MRJSV model dynamics, we have from (4) that

$$\begin{aligned} & E\left(\exp\left\{i\eta_n V_{n\delta} + i\vartheta_n X_{n\delta}\right\}|\mathcal{F}_{(n-1)\delta}\right) \\ = \ & \exp\left\{\psi_J(\delta,\vartheta_n) + \psi_0(\delta,\eta_n,\vartheta_n) + \psi_1(\delta,\eta_n,\vartheta_n)V_{(n-1)\delta} + \psi_2(\delta,\eta_n,\vartheta_n)X_{(n-1)\delta}\right\}, \end{aligned} \tag{A.7}$$

and for $j = n-1, n-2, \ldots, 1$

$$\begin{aligned} & E\left(\exp\left\{\psi_1(\delta,\eta_{j+1},\vartheta_{j+1})V_{j\delta} + \left(\psi_2(\delta,\eta_{j+1},\vartheta_{j+1}) + \frac{iu}{n+1}\right)X_{j\delta}\right\}\middle|\mathcal{F}_{(j-1)\delta}\right) \\ = \ & \exp\left\{\psi_J(\delta,\vartheta_j) + \psi_0(\delta,\eta_j,\vartheta_j) + \psi_1(\delta,\eta_j,\vartheta_j)V_{(j-1)\delta} + \psi_2(\delta,\eta_j,\vartheta_j)X_{(j-1)\delta}\right\}. \end{aligned} \tag{A.8}$$

Evaluating

$$E\left(e^{iuY_{n+1}}\right) = E\left(\exp\left\{\frac{iu}{n+1}\sum\nolimits_{j=0}^{n}X_{j\delta}\right\}\right)$$

using iterated expectations and applying equalities (A.7)–(A.8), we obtain (14).

(b) Define $Z_j = X_{j\delta} - X_{(j-1)\delta}e^{-k\delta}$, where $j = 1, \ldots, n$. By recursive substitution in $X_{j\delta} = X_{(j-1)\delta}e^{-k\delta} + Z_j$ and summation across all j, we get

$$\sum_{j=0}^{n} X_{j\delta} = X_0 + \sum_{j=1}^{n} \left\{ X_0 e^{-kj\delta} + \sum_{m=0}^{n-j} Z_j e^{-mk\delta} \right\}.$$

Then,

$$\begin{aligned} E\left(e^{iuY_{n+1}}\right) &= E\left(\exp\left\{\frac{iu}{n+1}\sum_{j=0}^{n} X_{j\delta}\right\}\right) \\ &= \exp\left\{\frac{iu}{n+1}\sum_{j=0}^{n} X_0 e^{-kj\delta}\right\} E\left(\exp\left\{\frac{iu}{n+1}\sum_{j=1}^{n} Z_j \sum_{m=0}^{n-j} e^{-mk\delta}\right\}\right) \\ &= \prod_{j=0}^{n} \exp\left\{\frac{iu}{n+1} X_0 e^{-kj\delta}\right\} \prod_{j=1}^{n} E\left(\exp\left\{i\eta_j Z_j\right\}\right), \end{aligned}$$

where the last equality follows by stochastic independence of the variables $\{Z_j\}_{j=1}^{n}$ and the characteristic function of Z_j from Eq. (9).

■

References

Ahlip, R., 'Foreign exchange options under stochastic volatility and stochastic interest rates', *International Journal of Theoretical and Applied Finance*, Vol. 11(3), 2008, pp. 277–294.

Andersen, L., 'Simple and efficient simulation of the Heston stochastic volatility model', *Journal of Computational Finance*, Vol. 11(3), 2008, pp. 1–42.

Bates, D.S., 'Jumps and stochastic volatility: exchange rate processes implicit in deutsche mark options', *Review of Financial Studies*, Vol. 9(1), 1996, pp. 69–107.

Benth, F.E., 'The stochastic volatility model of Barndorff-Nielsen and Shephard in commodity markets', *Mathematical Finance*, Vol. 21(4), 2011, pp. 595–625.

Bessembinder, H., Coughenour, J.F., Seguin, P.J. and Smoller, M.M., 'Mean reversion in equilibrium asset prices: evidence from the futures term structure', *Journal of Finance*, Vol. 50(1), 1995, pp. 361–375.

Borovkova, S. and Geman, H., 'Seasonal and stochastic effects in commodity forward curves', *Review of Derivatives Research*, Vol. 9(2), 2006, pp. 167–186.

Borovkova, S. and Permana, F., 'Modelling electricity prices by the potential jump-diffusion', in A. N. Shiryaev, M. R. Grossinho, P. E. Oliveira, M. L. Esquível, eds., *Stochastic Finance* (New York: Springer, 2006), pp. 239–263.

Branger, N., Krautheim, E., Schlag, C. and Seeger, N., 'Hedging under model misspecification: all risk factors are equal, but some are more equal than others...', *Journal of Futures Markets*, Vol. 32(5), 2012, pp. 397–430.

Broadie, M., Chernov, M. and Johannes, M., 'Model specification and risk premia: Evidence from futures options', *Journal of Finance*, Vol. 62(3), 2007, pp. 1453–1490.

Brooks, C. and Prokopczuk, M., 'The dynamics of commodity prices', *Quantitative Finance*, Vol. 13(4), 2013, pp. 527–542.

Carr, P. and Madan, D.B., 'Option valuation using the fast Fourier transform', *Journal of Computational Finance*, Vol. 2(4), 1999, pp. 61–73.

Carr, P. and Wu, L., 'Static hedging of standard options', *Journal of Financial Econometrics*, Vol. 12(1), 2014, pp. 3–46.

Casassus, J. and Collin-Dufresne, P., 'Stochastic convenience yield implied from commodity futures and interest rates', *Journal of Finance*, Vol. 60(5), 2005, pp. 2283–2331.

Černý, A. and Kyriakou, I., 'An improved convolution algorithm for discretely sampled Asian options', *Quantitative Finance*, Vol. 11(3), 2011, pp. 381–389.

Clewlow, L. and Strickland, C., *Energy Derivatives: Pricing and Risk Management* (London: Lacima Publications, 2000).

Cont, R. and Tankov, P., *Financial Modelling with Jump Processes* (Boca Raton: Chapman & Hall/CRC Press, 2004).

Duffie, D., Filipović, D. and Schachermayer, W., 'Affine processes and applications in finance', *The Annals of Applied Probability*, Vol. 13(3), 2003, pp. 984–1053.

Duffie, D., Pan, J. and Singleton, K., 'Transform analysis and asset pricing for affine jump-diffusions', *Econometrica*, Vol. 68(6), 2000, pp. 1343–1376.

Fabozzi, F.J., Shiller, R.J. and Tunaru, R.S., 'A pricing framework for real estate derivatives', *European Financial Management*, Vol. 18(5), 2012, pp. 762–789.

Fusai, G. and Meucci, A., 'Pricing discretely monitored Asian options under Lévy processes', *Journal of Banking & Finance*, Vol. 32(10), 2008, pp. 2076–2088.

Geman, H., *Commodities and Commodity Derivatives: Modeling and Pricing for Agriculturals, Metals and Energy* (Chichester: Wiley-Finance, 2005).

Geman, H. and Nguyen, V.N., 'Soybean inventory and forward curve dynamics', *Management Science*, Vol. 51(7), 2005, pp. 1076–1091.

Geman, H. and Roncoroni, A., 'Understanding the fine structure of electricity prices', *The Journal of Business*, Vol. 79(3), 2006, pp. 1225–1261.

Glasserman, P., *Monte Carlo Methods in Financial Engineering* (New York: Springer, 2004).

Hansen, P.R., 'A test for superior predictive ability', *Journal of Business & Economic Statistics*, Vol. 23(4), 2005, pp. 365–380.

Heston, S.L., 'A closed-form solution for options with stochastic volatility with applications to bond and currency options', *Review of Financial Studies*, Vol. 6(2), 1993, pp. 327–343.

Hilliard, J.E. and Reis, J., 'Valuation of commodity futures and options under stochastic convenience yields, interest rates, and jump diffusions in the spot', *Journal of Financial and Quantitative Analysis*, Vol. 33(1), 1998, pp. 61–86.

Jarque, C.M. and Bera, A.K., 'Efficient tests for normality, homoscedasticity and serial independence of regression residuals', *Economics Letters*, Vol. 6(3), 1980, pp. 255–259.

Kaeck, A. and Alexander, C., 'Stochastic volatility jump-diffusions for European equity index dynamics', *European Financial Management*, Vol. 19(3), 2013, pp. 470–496.

Kemna, A.G.Z. and Vorst, A.C.F., 'A pricing method for options based on average asset values', *Journal of Banking & Finance*, Vol. 14(1), 1990, pp. 113–129.

Larsson, K. and Nossman, M., 'Jumps and stochastic volatility in oil prices: Time series evidence', *Energy Economics*, Vol. 33(3), 2011, pp. 504–514.

Nomikos, N. and Andriosopoulos, K., 'Modelling energy spot prices: Empirical evidence from NYMEX', *Energy Economics*, Vol. 34(4), 2012, pp. 1153–1169.

Nomikos, N.K., Kyriakou, I., Papapostolou, N.C. and Pouliasis, P.K., 'Freight options: Price modelling and empirical analysis', *Transportation Research Part E: Logistics and Transportation Review*, Vol. 51, 2013, pp. 82–94.

Pindyck, R.S., 'Volatility and commodity price dynamics', *Journal of Futures Markets*, Vol. 24(11), 2004, pp. 1029–1047.

Politis, D.N. and Romano, J.P., 'The stationary bootstrap', *Journal of the American Statistical Association*, Vol. 89(428), 1994, pp. 1303–1313.

Routledge, B.R., Seppi, D.J. and Spatt, C.S., 'Equilibrium forward curves for commodities', *Journal of Finance*, Vol. 55(3), 2000, pp. 1297–1338.

Schwartz, E. and Smith, J.E., 'Short-term variations and long-term dynamics in commodity prices', *Management Science*, Vol. 46(7), 2000, pp. 893–911.

Schwartz, E.S., 'The stochastic behaviour of commodity prices: implications for valuation and hedging', *Journal of Finance*, Vol. 52(3), 1997, pp. 923–973.

Sullivan, R., Timmermann, A. and White, H., 'Data-snooping, technical trading rule performance, and the bootstrap', *Journal of Finance*, Vol. 54(5), 1999, pp. 1647–1691.

Trolle, A.B. and Schwartz, E.S., 'Unspanned stochastic volatility and the pricing of commodity derivatives', *Review of Financial Studies*, Vol. 22(11), 2009, pp. 4423–4461.

White, H., 'A reality check for data snooping', *Econometrica*, Vol. 68(5), 2000, pp. 1097–1126.

Zhang, P.G., 'An introduction to exotic options', *European Financial Management*, Vol. 1(1), 1995, pp. 87–95.

Table 1: Model calibration

This table presents the model calibration results. Panel A reports the estimated annualized parameters (standard errors in [ ]) of the predictable component (1) for each of the Brent Crude Oil (CB), Gasoil (GO), WTI Crude Oil (CL), Gasoline (HU) and Heating Oil (HO) markets (note that parameter δ_0 is estimated subject to $\min(S_t - f_t) = \min S_t$ to ensure positive $S_t - f_t$). Panel B reports the estimated annualized parameters (standard errors in [ ]) of the MRSV and MRJSV models. Panel C reports the error statistics computed for the entire term structure of futures prices: RRMSE $:= \sqrt{\frac{1}{mn}\sum_{j=1}^{n}\sum_{l=1}^{m}\left|F_{\theta^*}(t_j,T_l)/F_{j,l}-1\right|^2}$ and RMSE $:= \sqrt{\frac{1}{mn}\sum_{j=1}^{n}\sum_{l=1}^{m}\left|F_{\theta^*}(t_j,T_l)-F_{j,l}\right|^2}$, where $F_{j,l}$ is the observed futures prices at time t_j of a contract maturing at T_l, $F_{\theta^*}(t_j,T_l)$ is the theoretical futures price given in Proposition 1 for each model under optimal parameter set θ^* (see Eq. 10), $m = 12$ (no. of maturities) and $n = 1,043$ (no. of days in sample period March 12, 2009 to March 11, 2013). In addition, we test the null hypothesis that none of MRJ, MRSV and MRJSV models leads to reduction in futures pricing errors (RRMSE and RMSE) relative to the MR model, by employing the Hansen (2005) test and the stationary bootstrap of Politis and Romano (1994) using 5,000 bootstrap simulations. Asterisks (*) indicate significance at the 10% level.

	CB		GO		CL		HU		HO	
Panel A: predictable component parameters										
δ_0	–5.592 [1.217]		–40.64 [8.740]		–4.235 [1.305]		–0.187 [0.029]		–0.136 [0.038]	
δ_1	3.479 [0.362]		–20.56 [2.021]		3.871 [0.480]		0.156 [0.001]		–0.069 [0.001]	
τ_1	1.204 [0.042]		3.711 [0.055]		1.273 [0.067]		1.059 [0.020]		0.774 [0.011]	
δ_2	–2.406 [0.751]		–23.62 [0.403]		–0.877 [2.582]		0.06 [0.001]		0.062 [0.001]	
τ_2	1.836 [0.031]		–2.673 [0.024]		1.328 [0.101]		1.073 [0.028]		1.085 [0.067]	
δ_3	14.86 [0.576]		141.2 [4.339]		8.566 [0.914]		0.411 [0.012]		0.446 [0.021]	
Panel B: spot price & variance model parameters										
	MRSV	MRJSV	MRSV	MRJSV	MRSV	MRJSV	MRSV	MRJSV	MRSV	MRJSV
ε	4.252 [0.066]	4.253 [0.137]	6.318 [0.056]	6.319 [0.062]	4.279 [0.034]	4.281 [0.041]	0.608 [0.037]	0.609 [0.085]	0.554 [0.043]	0.559 [0.058]
k	3.563 [0.423]	3.344 [0.206]	3.281 [1.413]	2.999 [0.680]	5.002 [1.775]	4.278 [0.117]	6.385 [2.018]	4.703 [1.034]	4.088 [1.505]	3.221 [1.503]
λ	-	3.400 [0.751]	-	3.2 [0.540]	-	5.000 [0.526]	-	7.600 [1.064]	-	4.600 [0.417]
μ_J	-	–0.026 [0.016]	-	–0.013 [0.017]	-	–0.002 [0.015]	-	–0.007 [0.015]	-	–0.002 [0.016]
σ_J	-	0.064 [0.001]	-	0.067 [0.002]	-	0.077 [0.002]	-	0.092 [0.002]	-	0.079 [0.002]
h	0.599 [0.301]	0.389 [0.206]	0.643 [0.200]	0.533 [0.184]	0.223 [0.032]	0.215 [0.028]	1.101 [0.323]	0.983 [0.285]	0.546 [0.244]	0.530 [0.240]
α	36.68 [20.34]	31.52 [18.34]	30.71 [3.442]	16.76 [3.014]	37.33 [19.96]	21.920 [12.89]	84.23 [43.01]	52.32 [24.21]	42.12 [19.87]	40.33 [14.62]
β	0.263 [0.064]	0.230 [0.062]	0.349 [0.070]	0.245 [0.052]	0.315 [0.100]	0.216 [0.062]	0.700 [0.101]	0.478 [0.085]	0.350 [0.100]	0.344 [0.069]
γ	1.259 [0.600]	0.989 [0.546]	1.860 [1.090]	1.084 [0.633]	1.531 [0.770]	1.114 [0.633]	3.694 [2.001]	1.950 [1.109]	1.817 [1.055]	1.742 [1.033]
ρ	0.204 [0.211]	0.181 [0.226]	0.254 [0.224]	0.186 [0.167]	0.236 [0.212]	0.172 [0.177]	0.452 [0.602]	0.300 [0.326]	0.247 [0.268]	0.245 [0.242]
$\hat{V}_1$	0.208 [0.070]	0.186 [0.076]	0.262 [0.131]	0.196 [0.100]	0.24 [0.110]	0.178 [0.100]	0.498 [0.251]	0.359 [0.190]	0.266 [0.119]	0.262 [0.150]
Panel C: futures pricing errors										
	RRMSE	RMSE	RRMSE	RMSE	RRMSE	RMSE	RRMSE	RMSE	RRMSE	RMSE
MR	0.136	7.782	0.146	63.18	0.104	7.106	0.171	0.238	0.139	0.202
MRJ	0.131*	7.508*	0.142*	61.43*	0.103*	6.960*	0.162*	0.225*	0.134*	0.193*
MRSV	0.135	7.767	0.143*	61.89*	0.104	7.009	0.165*	0.229*	0.137*	0.197*
MRJSV	0.129*	7.499*	0.140*	61.33*	0.102*	6.957*	0.160*	0.223*	0.133*	0.192*

Table 2: True data-generating process testing

We test whether the proposed models (MR, MRJ, MRSV, MRJSV) can accurately represent the true price dynamics of each commodity (CB, GO, CL, HU, HO). The table reports the relative performance across models in terms of percentage number of simulated log-return statistics of a given type lying within the corresponding 90% bootstrap confidence interval of the empirical statistic. Table entries correspond to values in the range 0 to 1: e.g., a value of 0.750 indicates that in 75% of 100,000 simulation runs, the simulated statistic has been within the bootstrap confidence interval. Abbreviations: standard deviation (std), skewness (skew), kurtosis (kurt), 1st and 99th percentiles (perc1 and perc99) and expected shortfalls at the 1% and 99% levels (ES1 and ES99). In addition, for each simulation, we employ the two-sample Kolmogorov–Smirnov (K–S) test for equality of the empirical and model-implied log-return distributions and report the percentage number of times the null hypothesis cannot be rejected at the 10% significance level. Asterisks (*) highlight best relative performance across models.

	std	skew	kurt	perc1	perc99	ES1	ES99	K–S test
Brent Crude Oil (CB)								
MR	0.731	0.031	0.295	0.280	0.890	0.144	0.803*	0.621
MRJ	0.866	0.556*	0.513	0.708	0.951*	0.779	0.564	0.833
MRSV	0.789	0.223	0.963*	0.388	0.766	0.242	0.747	0.646
MRJSV	0.871*	0.515	0.787	0.744*	0.860	0.857*	0.509	0.884*
Gasoil (GO)								
MR	0.575	0.122	0.189	0.263	0.817	0.109	0.881*	0.565
MRJ	0.896*	0.556	0.530	0.608	0.937*	0.777	0.772	0.811
MRSV	0.788	0.577	0.720	0.282	0.862	0.266	0.857	0.724
MRJSV	0.767	0.606*	0.772*	0.696*	0.821	0.800*	0.786	0.928*
WTI Crude Oil (CL)								
MR	0.679	0.479	0.000	0.243	0.834	0.003	0.341	0.551
MRJ	0.855	0.474	0.222	0.621	0.868*	0.728*	0.763	0.770
MRSV	0.836	0.428	0.283	0.442	0.836	0.455	0.970*	0.619
MRJSV	0.876*	0.636*	0.446*	0.737*	0.829	0.693	0.901	0.821*
Gasoline (HU)								
MR	0.733	0.515	0.000	0.062	0.970*	0.009	0.204	0.597
MRJ	0.824	0.559	0.352	0.597	0.932	0.804	0.743	0.760
MRSV	0.788	0.595	0.814*	0.242	0.752	0.426	0.656	0.685
MRJSV	0.855*	0.755*	0.577	0.719*	0.908	0.819*	0.918*	0.801*
Heating Oil (HO)								
MR	0.514	0.487	0.000	0.213	0.937	0.004	0.408	0.357
MRJ	0.872	0.578	0.481*	0.568	0.974	0.642	0.846	0.804
MRSV	0.781	0.442	0.364	0.888*	0.956	0.548	0.948*	0.817
MRJSV	0.892*	0.701*	0.465	0.872	0.996*	0.672*	0.941	0.844*

Table 3: Control variate Monte Carlo (CVMC) simulation scheme

Summarized CVMC simulation scheme. **Inputs**: M: number of simulations; n: number of monitoring (averaging) dates; T: option time to maturity; δ: time spacing; $\tilde{K}$: deseasonalized strike price; r: continuously compounded risk free interest rate; spot price model params.: ε, k, σ, λ, μ_J, σ_J, h; stoch. variance model params.: α, β, γ, ρ; $E(G) := E(e^{-rT}(\exp(\sum_{j=0}^{n} X_j/(n+1)) - \tilde{K})^+)$: exact price of geometric Asian option (pre-computed using formula 15); b^*: optimal CV coefficient (pre-estimated using a pilot run, see Glasserman, 2004, Section 4.1.3). **Control Variate Monte Carlo**: simulation of MR model (step 1.b): exact method, e.g., see Glasserman (2004, Section 3.3); simulation of square-root diffusion (step 1.c): $\chi'^2_{df}(cV_{j-1})$ noncentral chi-square random variable with $df := 4\alpha\beta\gamma^{-2}$ degrees of freedom and noncentrality parameter cV_{j-1}, $c := 4\alpha e^{-\alpha\delta}\gamma^{-2}(1-e^{-\alpha\delta})^{-1}$, is simulated using the method described in Glasserman (2004, Section 3.4) (alternatively, for a faster simulation, the low-bias quadratic-exponential method of Andersen, 2008 can be used); simulation of MRSV model (step 1.d): modified Andersen (2008) method with central discretization employed in both integrated log-spot price and variance; simulation of compound Poisson process (step 2): improved algorithm in Cont and Tankov (2004, Section 6.1, Algorithm 6.2).

Inputs: M; n; T; $\delta \leftarrow T/n$; $\tilde{K}$; r; model params.; $E(G)$; b^*

CVMC simulation:

1. Generate log deseas. spot price (& stochastic variance) sample path:

1a. Generate n indep. normal variates $N_{01,j} \sim \mathcal{N}(0,1)$ for $j = 1, \ldots, n$

1b. Set $X_j \leftarrow X_{j-1}e^{-k\delta} + (\varepsilon - h/k)(1-e^{-k\delta}) + \sigma\sqrt{(1-e^{-2k\delta})/(2k)}N_{01,j}$ (MR)

1c. Set $V_j \leftarrow c^{-1}e^{-\alpha\delta}\chi'^2_{df}(cV_{j-1})$ for $j = 1, \ldots, n$

1d. Set $X_j \leftarrow [X_{j-1}(1-k\delta/2) + (k\varepsilon - h - \alpha\beta\rho/\gamma)\delta + V_{j-1}(\alpha\delta/2-1)\rho/\gamma$
$+V_j(\alpha\delta/2+1)\rho/\gamma + \sqrt{(1-\rho^2)(V_{j-1}+V_j)\delta/2}N_{01,j}\Big](1+k\delta/2)^{-1}$ (MRSV)

2. Generate independent compound Poisson process:

2a. Generate n indep. Poisson variates $N_{J,j} \sim$Pois$(\lambda\delta)$ for $j = 1, \ldots, n$

2b. Generate $N_{J,j}$ indep. normal variates $J_{j,i} \sim \mathcal{N}(\mu_J, \sigma_J^2)$ for $i = 1, \ldots, N_{J,j}$

2c. Generate $N_{J,j}$ indep. uniform variates $U_{j,i} \sim$ Unif$[0,\delta]$ for $i = 1, \ldots, N_{J,j}$

3. Generate log deseas. spot price path with jumps:

3a. Set $X_j \leftarrow X_j + \sum_{i=1}^{N_{J,j}} \mathbf{1}_{U_{j,i}<\delta} J_{j,i}$ (MR to MRJ)

3b. Set $X_j \leftarrow X_j + (1+k\delta/2)^{-1}\sum_{i=1}^{N_{J,j}} \mathbf{1}_{U_{j,i}<\delta} J_{j,i}$ (MRSV to MRJSV)

4. Generate option payoff samples:

4a. Set $C \leftarrow e^{-rT}\left(\sum_{j=0}^{n}\exp(X_j)/(n+1) - \tilde{K}\right)^+$ (arithmetic average)

4b. Set $G \leftarrow e^{-rT}\left(\exp\left(\sum_{j=0}^{n} X_j/(n+1)\right) - \tilde{K}\right)^+$ (geometric average)

4c. Set $C_b \leftarrow C - b^*(G - E(G))$ (control variate)

5. Repeat steps 1–4 for all M simulations

6. Return option price estimate $E(C_b) \leftarrow \frac{1}{M}\sum C_b$

7. Return standard error $\frac{1}{M-1}\sum (C_b - E(C_b))^2$

Table 4: Arithmetic Asian option prices

This table reports the price estimates of at-the-money (ATM), in-the-money (ITM) and out-of-the-money (OTM) 1-month to maturity arithmetic Asian call options with daily averaging, obtained by implementing the control variate Monte Carlo simulation approach in Section 5.1 (see also Table 3) with 100,000 simulations, for each model (MR, MRJ, MRSV, MRJSV) and market (CB, GO, CL, HU, HO). The strike price is set equal to 100%, 95% and 105% of the spot price, resp., ATM, ITM and OTM options. The current spot price and variance are set equal to $\exp(\varepsilon)$ and β, respectively. Columns 2–4 report option prices, columns 5–7 option prices relative to the spot price (%), columns 8–9 ITM and OTM option prices relative to the price of the corresponding ATM option (%).

	Option prices			Relative to spot (%)			Relative to ATM (%)	
	ITM	ATM	OTM	ITM	ATM	OTM	ITM	OTM
Brent Crude Oil (CB) - spot price 70.32 $/bbl								
MR	2.68	0.84	0.16	3.81	1.20	0.23	318	19
MRJ	3.01	1.02	0.22	4.28	1.46	0.31	294	21
MRSV	3.27	1.48	0.55	4.65	2.11	0.78	220	36
MRJSV	3.51	1.62	0.60	4.99	2.30	0.86	216	37
Gasoil (GO) - spot price 554.80 $/mt								
MR	20.87	6.62	1.31	3.76	1.19	0.24	315	19
MRJ	22.26	7.41	1.61	4.01	1.34	0.29	300	21
MRSV	27.75	13.82	6.11	5.00	2.49	1.10	201	44
MRJSV	27.54	13.49	5.58	4.96	2.43	1.01	204	41
WTI Crude Oil (CL) - spot price 72.26 $/bbl								
MR	3.65	1.36	0.33	5.05	1.88	0.45	268	23
MRJ	3.70	1.42	0.38	5.12	1.97	0.53	259	26
MRSV	4.21	2.10	0.89	5.83	2.90	1.24	200	42
MRJSV	4.20	2.05	0.85	5.81	2.83	1.17	205	41
Gasoline (HU) - spot price 184 c$/gal								
MR	5.6	1.9	0.5	3.02	1.05	0.27	287	25
MRJ	6.7	2.6	0.8	3.64	1.42	0.45	257	31
MRSV	10.1	5.8	3.3	5.47	3.15	1.77	173	56
MRJSV	9.7	5.5	3.0	5.28	3.02	1.61	175	53
Heating Oil (HO) - spot price 175 c$/gal								
MR	7.1	2.5	0.6	4.08	1.42	0.33	287	23
MRJ	7.5	2.8	0.8	4.31	1.60	0.43	269	27
MRSV	9.3	4.7	2.1	5.30	2.66	1.19	199	44
MRJSV	9.4	5.0	2.3	5.39	2.85	1.31	189	45

Table 5: Hedging performance comparisons

Panel A reports for each market the mean and standard deviation (std) of the simulated hedging error at the closing of a week-long dynamic delta strategy with daily rebalancing without model misspecification in monetary terms (CB - \$/bbl, GO - \$/mt, CL - \$/bbl, HU - \$/gal, HO - \$/gal). Panel B reports % increases (positive signs) in the standard deviation of the hedging error when the hedge portfolios are misspecified, in particular, the incorrect hedge models contain fewer risk factors than the true model. Hedging error is defined as the difference between the value of the daily-rebalanced hedge portfolio and the value of a 1-month to maturity, daily-averaged ATM arithmetic Asian option for the 1-week hedge period.

	CB	GO	CL	HU	HO
Panel A: hedges without model misspecification					
(1) MR hedging error					
mean	–0.195	–1.711	–0.048	–0.008	–0.003
std	0.294	2.349	0.308	0.011	0.008
(2) MRJ hedging error					
mean	–0.229	–1.925	–0.052	–0.009	–0.005
std	0.364	3.319	0.518	0.017	0.012
(3) MRSV hedging error					
mean	–0.212	–1.870	–0.100	–0.009	–0.004
std	0.450	4.280	0.509	0.020	0.013
(4) MRJSV hedging error					
mean	–0.236	–1.988	–0.102	–0.010	–0.006
std	0.493	4.079	0.547	0.020	0.016
Panel B: % changes in std of hedging error under model misspecification (less risk factors)					
(1) true MRJ model					
MR	2.24	1.32	0.27	8.53	1.18
(2) true MRSV model					
MR	5.67	10.63	1.02	28.72	9.06
(3) true MRJSV model					
MR	4.40	4.84	1.15	18.34	5.21
MRJ	2.49	3.65	0.41	5.55	5.66
MRSV	2.69	0.05	0.41	2.61	1.10

Fig. 1: Simulated commodity price paths and hedging error distributions

Simulated (deseasonalized) price paths of each underlying commodity (panel a: CB - \$/bbl, panel b: GO - \$/mt, panel c: CL - \$/bbl, panel d: HU - \$/gal, panel e: HO - \$/gal) across a 5-day hedge period coupled with the distributions (Matlab's kernel smoothing function estimates) of the hedging errors at the closing of a week-long dynamic delta strategy with daily rebalancing without model misspecification, under the four data-generating processes (i: MR, ii: MRJ, iii: MRSV, iv: MRJSV). Hedging error is defined as the difference between the value of the daily-rebalanced hedge portfolio and the value of a 1-month to maturity, daily-averaged ATM arithmetic Asian option for the 1-week hedge period.

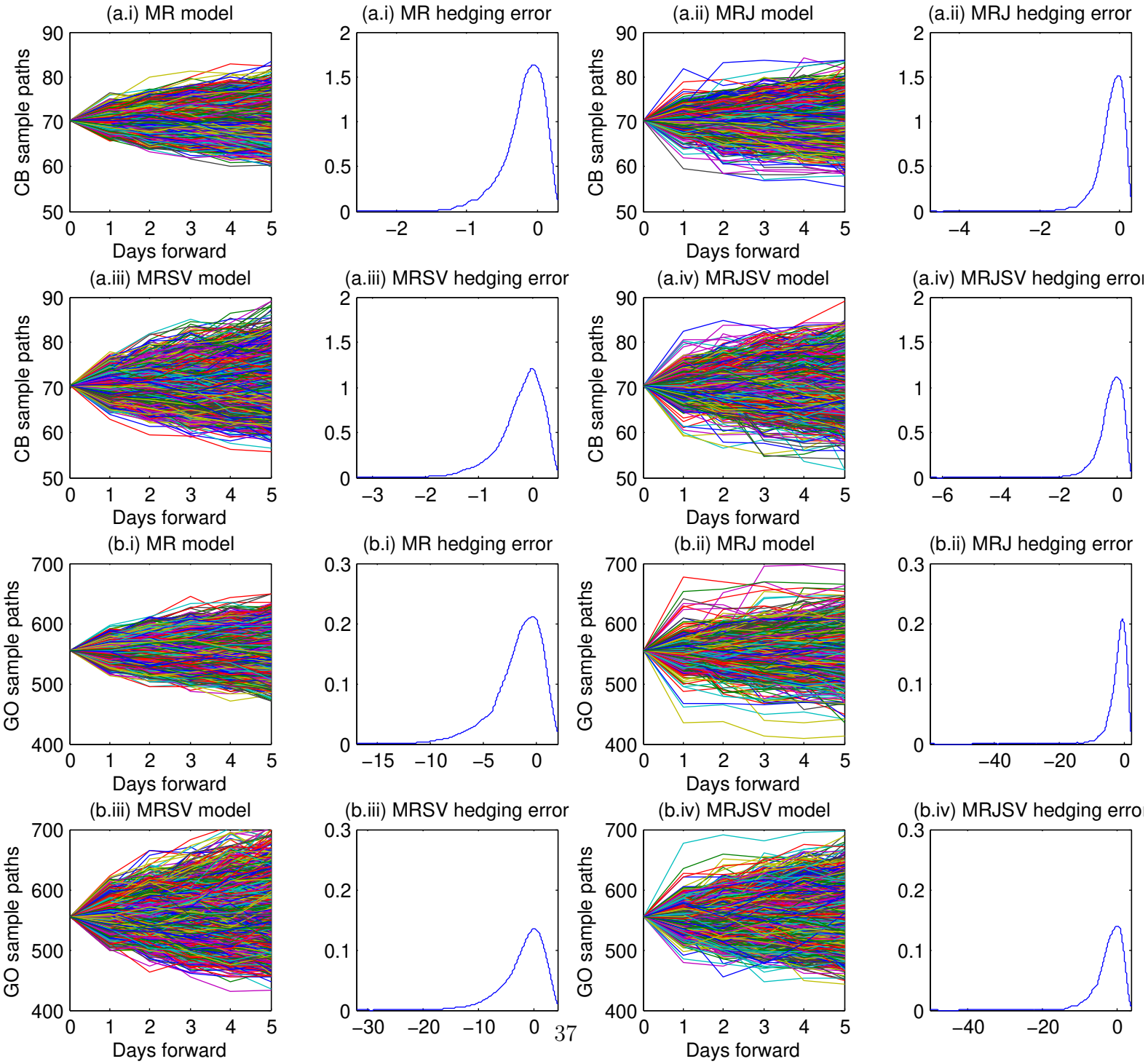

Fig. 1 continued

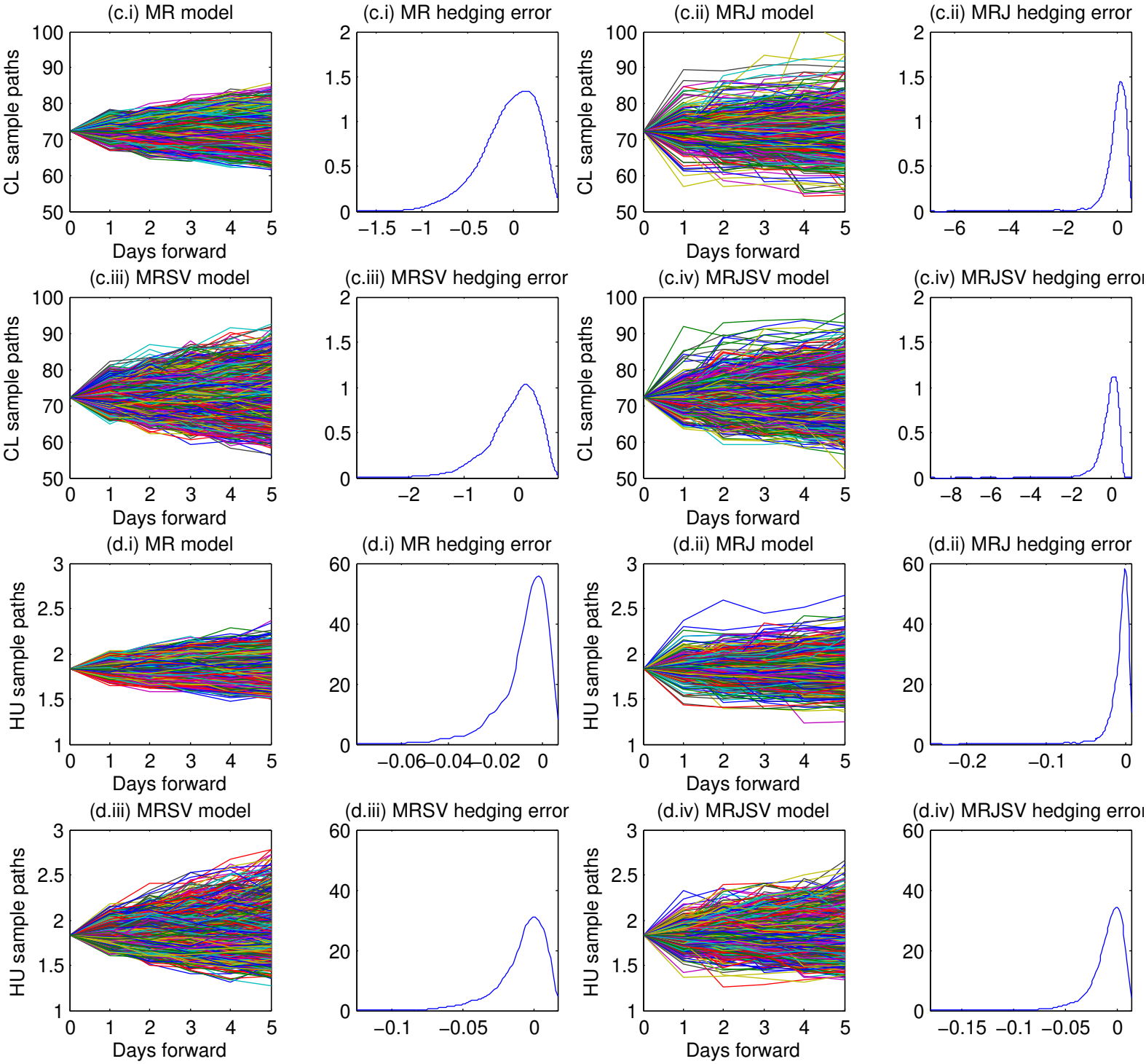

Fig. 1 continued